Studies of allosteric coupling in KcsA using a constitutively open mutant

Zhiyu Sun[a], **Yunyao Xu**[a], **Dongyu Zhang**[a], **and Ann E. McDermott**[a,1]

[a]Department of Chemistry, Columbia University, New York, NY, 10027

This manuscript was compiled on March 5, 2019

The transmembrane allosteric coupling in the c-type inactivation mechanism of a potassium channel is analyzed using NMR. Activation of KcsA is initiated by a decrease in pH on the intracellular side of the channel. Numerous studies suggest that the selectivity filter is subsequently allosterically affected by opening and that a conformational switch and loss of affinity for potassium ions is the central step of c-type inactivation. We tested this hypothesis using an open pH gate KcsA mutant (H25R/E118A) which is constitutively open and lacks pH-dependent behavior of the activation gate. We present Solid State NMR measurements of this open pH gate mutant at neutral pH and probe its potassium concentration dependence. The potassium binding affinity of the selectivity filter is 81 mM, about 4 orders of magnitude weaker than for the wild type KcsA at neutral pH, but similar to the value for wild type KcsA at low pH. The protonation state of an important glutamate residue (E120) in the pH sensor of the activation gate changes as a function of potassium concentration, indicating that this mutant also exhibits transmembrane allosteric coupling.

Solid State NMR | potassium channel | allostery | electrophysiology

Potassium channels selectively permit potassium ions to flow across biological membranes upon activation by an external stimulus such as voltage or nucleotide binding. Potassium channels typically contain a selectivity filter, which selects for potassium over other ambient ions with high affinity, as well as an activation gate that opens the channel and initiates the flow of potassium. In many potassium channels, however, the channel spontaneously stops conduction even when potassium ions and activation stimuli are still present (1, 2). This process typically occurs on a millisecond timescale after activation and is termed C-type inactivation. Inactivation has slow kinetics and is highly modulated by permeant ions and pore blockers (3). Understanding the structural basis of C-type inactivation is crucial to depict the regulation and drug response mechanism of biomedically important channels (4, 5).

KcsA is a prototypical bacterial potassium channel which is pH-activated. The pH gate is located at the intracellular face of the channel, formed by a group of key ionizable residues including H25, E118 and E120 (6–8). Like its more complex eukaryotic homologs, KcsA undergoes inactivation on the millisecond timescale after activation by a drop of pH (6, 9). In previous studies, our and other groups hypothesized that the site of inactivation is in the selectivity filter, where potassium ions are bound and conducted through the membrane (1, 10–12) . This mechanism is termed activation-coupled inactivation, i.e., and proposes that an allosteric coupling between the selectivity filter and activation gate (like the pH gate in KcsA) lead to a decrease in potassium affinity at the selectivity filter after activation. A direct measurement of the potassium ion affinity at the selectivity filter by solid state nuclear magnetic resonance (SSNMR) was done on KcsA embedded in authentic lipid environment (13). The result showed that the potassium ion affinity changed from $K_{apparent}$ = 14 ś 1 mM at pH 3.5 to 4 ś 1 M at pH 7.5. After activating the channel at low pH, the potassium affinity reduction at the selectivity filter essentially leads to ion loss and conformational change at the selectivity filter, which will cause a low level of potassium ion flow through the channel. This is consistent with the finding via electrophysiology that increasing extracellular potassium ion concentration could decrease the rate of inactivation (10, 12).

To further investigate the allosteric coupling between the pH gate and the selectivity filter, in this study, we aim to affirm this conclusion by showing that a mutation which cause opening of the pH gate at a neutral pH (a deactivation pH) also leads to a lower affinity at the selectivity filter. We achieved this by utilizing a KcsA mutant whose pH gate is open at neutral pH. Multiple studies have shown that there is a network of ionizable residues, including Histidine 25, Glutamic acid 118 and 120. These residues have been suggested to form complex inter- and intra-subunit interactions at the cytoplasmic ends of the TM1 and TM2 transmembrane helices (14–16). By mutating H25R, E118A and E120A, the pH gate remains open from pH 4 to 9 (17). This result is consistent with the finding by solution NMR data showing H25 is a pH sensor (18). A study was done to find the minimal number of amino acids mutated to open the pH gate and the authors found that the H25R and E118A are the essential two mutations (19).

Results

Mutation at the pH gate does not directly change the conductive/collapsed conformation at the selectivity filter. NMR chemical shifts are precise indicators for protein structural and conformational changes. We conducted solid-state NMR

Significance Statement

Opening of the activation gate causes subsequent constriction of the selectivity filter in the potassium channel, KcsA, controlling its mean open time and activity. In this study an open pH gate KcsA mutant was used for solid state NMR studies at neutral pH in bilayers. The potassium binding affinity is weak, providing strong evidence that opening of potassium channels leads to their loosening their grip on the potassium ions at the selectivity filter.

Author contributions: Z.S., Y.X. and A.E.M. designed research; Z.S., Y.X., D.Z. performed research; Z.S., Y.X. and A.E.M. analyzed data; Z.S., Y.X., and A.E.M. wrote the paper.

The authors declare no conflict of interest.

[1]To whom correspondence should be addressed. E-mail: aem5@columbia.edu

DRAFT

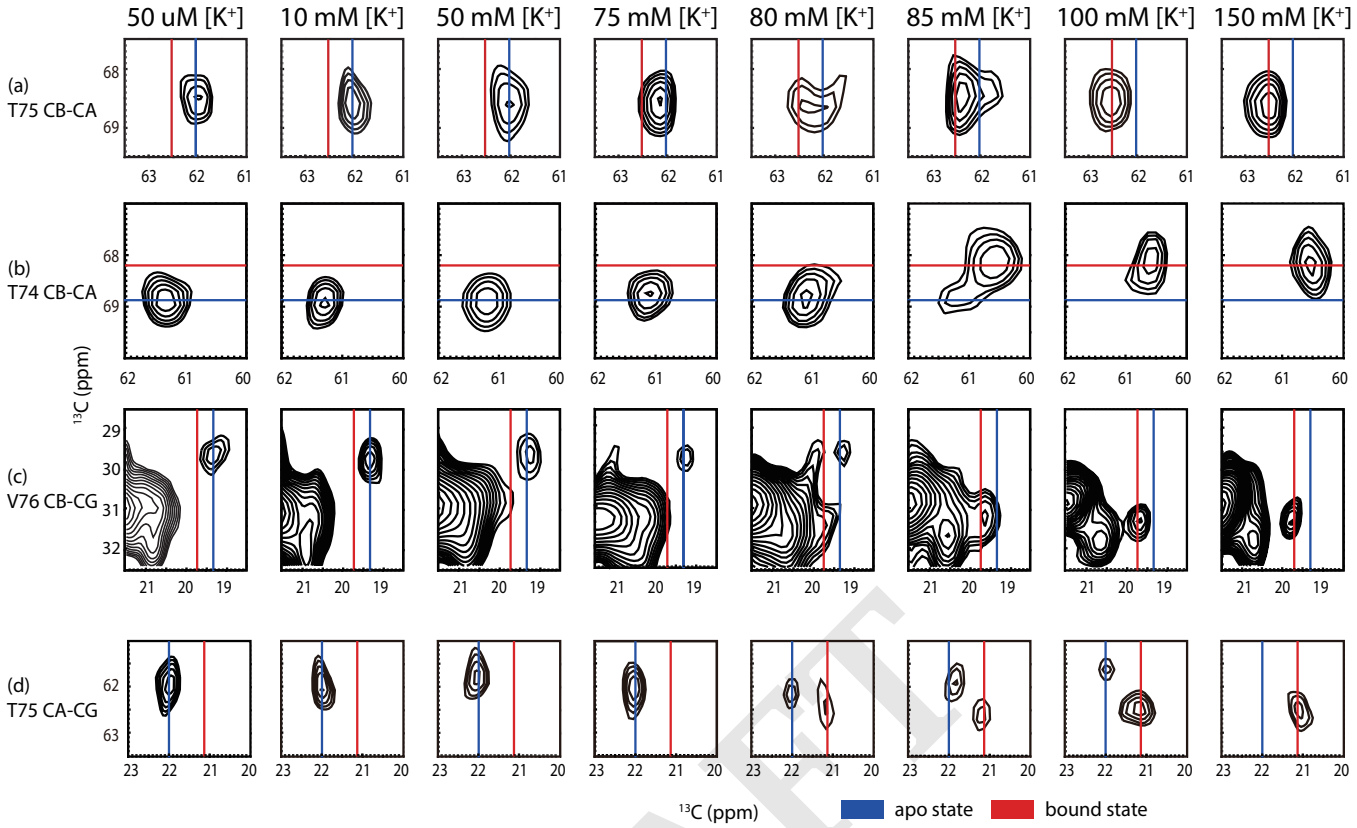

Fig. 1. [K^+] dependence of the intensities of the apo and bound state cross peaks of marker peaks near the selectivity filter in 2D 13C-13C (a-d) correlation spectra of H25R/E118A KcsA at pH 7.5. (a) T75 CB-CA. (b) T74 CB-CA. (c) V75 CB-CG. (d) T75 CA-CG. (a-d) show that the marker peaks shift from apo state in low [K+] to bound state in high [K+]. The contour level of the spectrum were set at 5 times noise level. Marker peaks could be integrated to calculate the population ratio of apo and bound states.

DRAFT

experiments to investigate the structure of H25R/E118A mutant in the lipid bilayer environment (DOPE:DOPS = 9:1) with 1:1 protein to lipid ratio, analogously to our prior studies (13). As seen in Figures S1 and S2, the protein is well folded and displays high-quality NMR spectra at both the low (3.5) and high (7.5) pH where most markers are similar to the wild type. This confirms that H25R/E118A mutant is well folded in lipid bilayers. Moreover, the H25R/E118A mutant displays two conformations at the selectivity filter, analogously to the wild type. NMR chemical shifts report the conformational change that occurs during K^+ binding for the wild type, as has been extensively discussed in relation to the two major conductive and collapsed conformations seen in various crystal structures. Two sets of chemical shifts of the H25R/E118A mutant are observed for the selectivity filter in different [K^+], at both pH values. This indicates that H25R/E118A mutants do not directly cause a new conformation at the selectivity filter, which is consistent with that H25 and E118 have been shown to be proton binding sites.

Opening the pH gate significantly lowers potassium affinity at the selectivity filter at neutral pH. To probe the allosteric coupling between the pH gate and the selectivity filter, we determined the potassium affinity of the open pH gate mutant H25R/E118A KcsA at neutral pH. As discussed above, E118&H25R mutant displays the K^+-bound (i.e. conductive) and K^+-apo (i.e. collapsed or inactivated) conformation. We used residues previously shown to have characteristic chemical shifts in the potassium binding site including T75 (CA, CB, CG), T74 (CA ,CB, CG), V76 (CA, CG) to assign the apo and K^+ bound population. The detailed cross peaks of marker peaks near the selectivity filter in 2D ^{13}C-^{13}C DARR spectra under 10, 50, 75, 80, 85, 100, 150 mM [K^+] were shown in Figure 1. (a-c). At intermediate [K^+], both the apo and bound peaks have significant intensities, indicating that the equilibrium of open and collapsed states of the open pH gate KcsA mutant is near these conditions. Also, no intermediate NMR lines are present at these conditions, indicating the conformations are in the slow exchange regime, characteristic of a bimodal conformational distribution, which is consistent with previous measurements for wild type KcsA, indicating that these mutations at the pH gate do not have a substantial change to the dynamics of the structural transition at the selectivity filter (13).

The NMR spectra showed that the KcsA channels were in the activated and inactivated states, and bound ratio against [K^+] could be fit to a Hill model. From the model fitting $K_{apparent}$ was extracted (13). When Vmax is set to 1 and Hill coefficient is set free, the $K_{apparent}$ of H25R/E118A KcsA was best fit to 81 ś 1 mM in contrast with 4 ś 1 M for wild type KcsA at pH 7.5 and 14 ś 1 mM for wild type KcsA at pH 3.5 (Figure 2). Details of the Hill fit were shown in Table. S1. An interesting observation from the titration curve for the H25R&E118A mutant is that the transition from the bound to the unbound

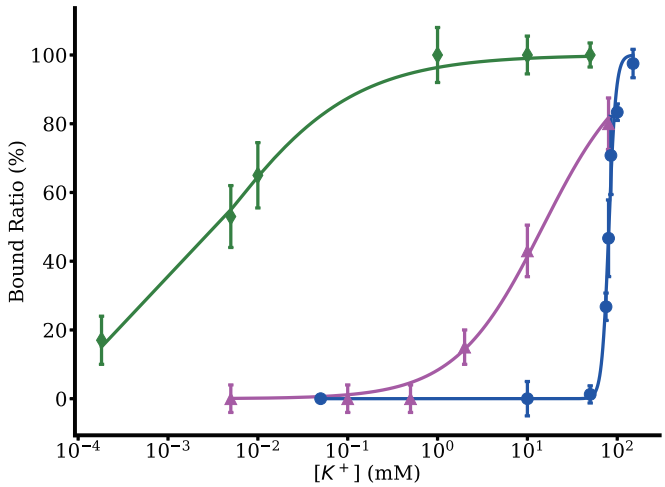

Fig. 2. The bound ratio is plotted against [K$^+$] to make the titration graph. The H25R/E118A (blue) is compared with our former data of wild type pH 7.5 (green) and wild type pH 3.5 (magenta). $K_{apparent}$ of the open pH gate mutant was calculated to be 81 ś 1 mM by fitting the data to a Hill binding model compared with 4 ś 1 M for wild type at pH 7.5 and 14 ś 1 mM for wild type at pH 3.5 [13]. Our data show that keeping the pH gate open with H25R/E118A mutant further shift the K+ affinity to a lower level.

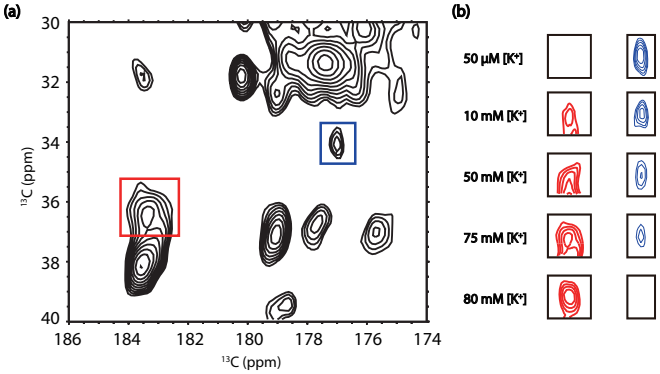

Fig. 3. The effect of [K$^+$] on E120 residue in the pH gate of the H25R/E118A KcsA mutant. 2D 13C-13C correlation spectrum of open pH gate KcsA at 75 mM [K$^+$] is shown in (a). The peaks in the red and blue rectangles are the E120 CG-CD peaks in deprotonated and protonated state respectively. The protonated and deprotonated state change of the E120 peak across various [K$^+$] is shown in (b). Protonated and deprotonated E120 CG-CD peaks at 50 M, 10, 50, 75 and 80 mM are shown. At pH 7.5, E120 is protonated at low [K$^+$], while at and above 80 mM [K$^+$], E120 is completely deprotonated. In samples with [K$^+$] larger than 80 mM, the E120 CG-CD peaks are all in the deprotonated state. This protonation state change provides clear evidence for pKa change of the glutamic acid residue.

state is very steep comparing to those for sample at pH7.5 and pH 3.5. We interpret this as an increasing in the cooperativity during the potassium ion binding at the selectivity filter. However, the system is complicated in terms of proton binding and potassium binding and the coupling between them, which prevent us from drawing a clean conclusion on this observation.

H25R/E118A mutant remains similar potassium affinity under low pH. To further validate that the affinity reduction caused by mutation of H25R/E118A and application of low pH is through allosteric effect. The bound ratio of mutant at 80 mM [K$^+$] is around 40%, which showed that the $K_{apparent}$ of the mutant at low pH was very close to the value at neutral pH (Figure S3). The little affinity difference confirms that after the pH gate is open in the H25R/E118A mutant, lowering pH does not further perturb the apo and bound population at the selectivity filter, indicating that these two perturbations affect the thermodynamics at the selectivity filter through similar coupling effect between the pH gate and the selectivity filter.

pH gate is coupled. Allosteric coupling between the selectivity filter and the pH gate was demonstrated in work (13, 20–25). Namely, not only does protonation and opening cause ion loss at the selectivity filter, but also protonation of the pH gate residues E118 and E120 is caused by selectivity filter pinching. In these spectra the peaks for E118 and E120 are congested and unresolved (13, 26). In the H25R/E118A mutant, we monitored the spectra of E120 during the K$^+$ titration process, as shown in Figure 3. The E120 CG-CD peak indicated that this residue is protonated at low [K$^+$],and deprotonated at high [K$^+$] (Figure 3a). The intensity of the protonated peak of E120 CG-CD decrease but the intensity of the deprotonated peak increase with increasing [K$^+$] (Figure 3b). At 50 M [K$^+$], E120 CG-CD appears to be essentially fully protonated, while at 80 mM [K$^+$] the E120 CG-CD appears to be essentially fully deprotonated. Curiously, the titrrration curve for E120 is not identical to that of the selectivity filter markers, suggesting K$^+$ ion sites of different affinity. These results show that in the H25R/E118A KcsA mutant, the pH gate and selectivity gate are coupled allosterically, and analogously to the wild type KcsA result (26).

Electrophysiology of the H25R/E118A mutant. It was previously shown that although the H25R/E118A mutant is open it does not conduct under standard electrophysiology conditions (pH 7.0, 100 mM [K$^+$]), because it, like the wild type, inactivates when open. But inactivation is suppressed by preparing the triple mutant E71A/H25R/E118A (24). We recently identified several participants in this allosteric process using NMR (27) and the results are in good agreement with prior molecular dynamics and electrophysiology studies (27, 28). These studies indicate that T74 is one of the important allosteric participants and that a mutation T74S causes a strong reduction in allosteric coupling in KcsA at pH 5.0 and pH 3.5. We reasoned therefore that the T74S/H25R/E118A mutant recovers about 30% of activity suggesting that when channels are opened by mutation, the T74S mutation reduces but does not obliterate the allosteric coupling (Figure 4). This result provides further support for the hypothesis that the H25R/E118A mutant has an open pH gate at neutral pH, and also supports our former hypothesis that T74 is important for allosteric coupling between the pH gate and the selectivity filter inactivation switch. The fact that E71A essentially abolishes allosteric coupling when coupled to the wild type pH sensor, whereas the T74S/H25R/E118A triple mutant partially inactivates suggests that these mutations in the pH gate causes subtle differences in the energetics of selectivity filter compared to the protonated wild type. It is interesting to speculate that, lacking the restraint of the hydrogen bonding network present in the wild type, the mutant may open to a greater degree and thereby encourage inactivation.

DRAFT

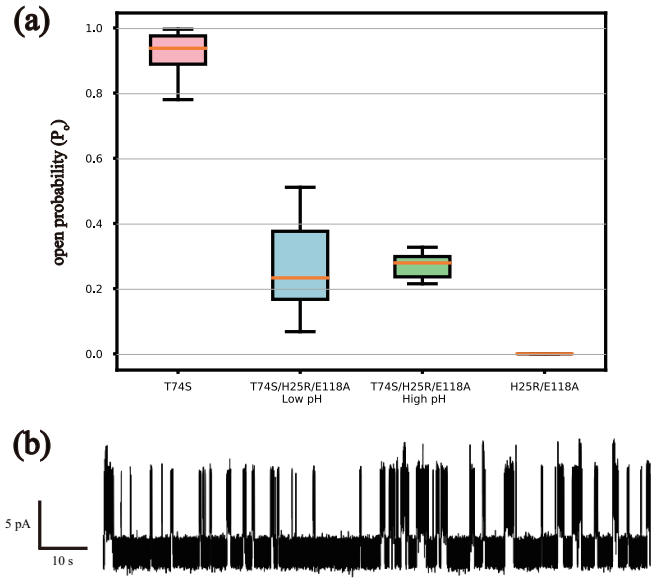

Fig. 4. Electrophysiology of open pH mutant and T74S triple mutant. (a). box plot of channel open probability. Open probability of T74S, H25RE118A_T74S low pH, H25RE118A_T74S high pH and H25RE118A are 90 ś 10%, 30 ś 20%, 27 ś 4% and 0 ś 0%. The pH of both H25RE118A_T74S buffer in the upper chamber are 7, but the pH of bath buffer in the chamber are 4 and 7 corresponding to low and high pH. (b). A trace of single channel T74S/H25R/E118A at +100 mV. The channel is 30% open compared to the 0% Po of inactivated H25R/E118A, which suggests that the allosteric coupling between the dual gates are attenuated by the T74S mutation.

Discussion

We used the open pH gate KcsA mutant H25R/E118A to study allosteric coupling in the inactivation process. Tetrametric KcsA was reconstituted in lipid bilayers and structural fingerprints were deciphered by SSNMR experiments. In the four-state scheme of KcsA, C-type inactivation develops when the channel reaches the activated state, with conductive selectivity filter and open pH gate, and the resulting state of the channel is inactivated, with collapsed selectivity filter and open pH gate (29, 30). By performing SSNMR experiments on open pH gate KcsA samples at different potassium concentrations, this transition pathway was reproduced. First, specific marker peaks at the selectivity filter were used to determine the percentage of bound population in the inactivation process. The titration study showed that the potassium ion affinity of the KcsA mutant shifted to 80 mM. Second, the pKa change of E120 residue at the pH gate showed that the pH gate was under strong allosteric coupling to the selectivity filter.

Because of the C-type inactivation, potassium channels in the activated state spontaneously undergo inactivation and are hard to capture for structural characterization under mild conditions (29). Efforts to trap the two states of the C-type inactivation process have often lowering the pH (22, 24, 26, 31–34). Although lowering the pH seems to be an intuitively correct method to trap the activated and the inactivated state, we had concerns about nonspecific effects of low pH (on both lipids and protein). At physiological condition, lipids are critical to sustain the function of KcsA by stabilizing specific conformation of it (35–38). Taking measurements on a mutant KcsA with constitutively open pH gate under physiological pH condition effectively eliminates this problem. The four orders of magnitude reduction on potassium affinity at the selectivity filter for H25R/E118A KcsA at neutral pH (81 mM vs. 6M) clears out our initial concern that the large affinity observed in the wild type KcsA at different pH is an artifact due to detrimental effect of low pH on the lipid or protein.

Our titration study shed light on allosteric coupling interactions in the inactivation process. It confirms that opening the pH gate, even though does not directly affect the bound and apo structures of the selectivity filter, significantly affect the populations of the two conformations, and biases the apo conformation. Since the pH gate and the selectivity filter is almost 30 Å away, such a dramatic effect is presumably through an allosteric coupling effect. We notice that experimental results from isothermal titration calorimetry (ITC) study on a similar mutant H25R/E118A/E120A with truncated C-terminus in a detergent environment show that the affinity for K^+ at pH 8 is 0.13 mM, close to the apparent potassium affinity value 0.15 mM for wild type KcsA in their measurement (39) . We attribute this inconsistency mostly to the usage of detergent in the experiment, which could potentially affect the structure and functions of membrane protein, as shown in study of KcsA and many other systems (1, 40). Truncation of the C-terminus certainly changes the thermodynamics properties of the channel; in electrophysiology experiment, KcsA with truncated C-terminus showed a more rapid and complete inactivation (29, 41). Therefore we believe solid state NMR measurement of full length KcsA with an environment of no detergent could better illustrate properties of the channel under near-physiological condition.

The potassium channel two-state conformation change during the inactivation process was characterized by two sets of chemical shifts at various potassium concentrations. The potassium affinity of the open pH mutant is in the same order of magnitude as the affinity of wild type KcsA channel under acidic condition. This result further confirms our allostery hypothesis, in C-type inactivation an open pH gate would strongly bias the selectivity filter towards the collapsed conformation. The pKa of the E120 at the intracellular pH gate was also shown to be under the influence of potassium ion binding at the selectivity filter, which provides additional evidence for an allosteric coupling network.

Materials and Methods

Expression and Purification of ^{13}C, ^{15}N-labeled open pH gate KcsA. The open pH gate H25R E118A KcsA was expressed with a plasmid kindly given by Crina Nimigean lab as a gift. The protein expression and purification protocol were based on our former work with minor modifications. 4 l of the open pH gate KcsA plasmids was added into 50 l JM83 competent cells in a culture test tube. The mixture was incubated on ice for 30 minutes, then heat-shocked for 70 seconds on a 42 ^{o}C water bath and incubated on ice for another 3 minutes. 1 mL of S.O.C recovery medium (Invitrogen) was added, and the cells were incubated at 37 ^{o}C for 1 hour. The transformed cells were plated up to Luria broth (LB) agar plates containing 100 g/ml ampicillin and incubated overnight at 37 ^{o}C. Single colonies of the transformed cells were picked and transferred to 4Œ 5 ml LB with 100 g/ml ampicillin. The preculture was incubated at 37 ^{o}C , 250 rpm, when the OD600 reached 1.0, the precultures were transferred into 4Œ 1 L LB with 100 g/ml ampicillin under same incubation condition. Once the OD600 reached 0.9, the cells were harvested via centrifugation at 4 ^{o}C, 8000 rpm for 15 minutes and resuspended in 1 L M9 medium with 3.0 g ^{13}C-labeled D-glucose,

DRAFT

0.5 g $^{15}NH_4Cl$ and 100 g/ml ampicillin. The cells were incubated at 37 ^{o}C, 250 rpm for 1 hour to recover. The protein expression was induced with anhydrotetracycline (Sigma), and incubated at 20 ^{o}C, 330 rpm overnight. The induced cells were harvested via centrifugation at 4 ^{o}C at 8000 rpm for 15 minutes, resuspended in 100 mM KCl, 50 mM Tris, 2 mM decyl maltoside (DM), pH 7.5 equilibrium buffer and lysed by French Press. The cell membranes were extracted with 30 mM DM at 4 ^{o}C overnight. The unlysed cells and membranes were pelleted via centrifugation at 4 ^{o}C at 15000 rpm for 1 hour. The protein was purified by nickel affinity column and eluted with 200 mM Imidazole. Imidazole concentration was reduced by dialysis against the equilibrium buffer, and the protein solution was concentrated for reconstitution.
9:1 w/w DOPE and DOPS (Avanti) were mixed in large test tube, the chloroform was evaporated by nitrogen gas flow, and the lipids was resuspended into 100 mM KCl, 50 mM Tris, 2 mM DM, 0.01 mM sodium azide, pH 7.5 buffer at concentration of 10 mg/ml. The ^{13}C,^{15}N-labeled open pH mutant KcsA was reconstituted into DOPE/DOPS liposome at 1:1 protein to liposome weight ratio. The mixture solution was dialyzed against a solution of 50 mM Tris, x mM KCl , (100-x) mM NaCl (to compensate ionic strength, except for the 150 mM KCl sample) at pH 7.5 overnight for three times under room temperature. The protein/liposome pellets were harvested, then freezed and thawed at 80 ^{o}C and room temperature for three times to remove bulk water. The final sample was reduced to a volume of around 30 l by doing three times of -80 ^{o}C to room temperature freeze-thaw cycle and packed into a 3.2 mm Bruker rotor, which corresponds to 10 mg mutant KcsA.

Solid-State Nuclear Magnetic Resonance and data analysis. Magic-angle-spinning (MAS) solid-state NMR spectra were measured on Bruker 750 MHz (17.6 T) and 900 MHz (21.1 T) Avance spectrometer in New York Structural Biology Center (NYSBC). The MAS rate was set to 14 kHz and the variable temperature apparatus was set to 264 K. Typical radiofrequency (rf) field strengths were 93-109 kHz for 1H and 50-62.5 kHz for 13C. 13C chemical shifts were referenced externally to the downfield adamantane CH2 resonance chemical shift at 40.48 ppm (42). 2D 13C-13C Dipolar Assisted Rotational Resonance (DARR) experiments were measured to obtain 13C chemical shifts (43, 44). The DARR mixing time was set at 15 ms. SPINAL64 decoupling on the 1H channel was set at 85-90 kHz during acquisition (45).
We calculated the population of the bound and apo states by integrating according cross peaks as previously did (13), the population of bound and apo state of marker peaks T75 CB-CA, T74 CB-CA, T75 AB-CG and V76 CB-CB were quantified by the intensity of the bound and apo state cross peaks by a sum over box method in sparky (46). The spectra were processed in Sparky : peaks were picked according to former assignment (26, 46), and the integral (I) of the 2D peaks were integrated using a sum over box method, so that the bound population =

$$\frac{I_{\text{bound}}}{I_{bound} + I_{\text{apo}}} \times 100\%$$

. The normalized bound ratios of the protein under different K^+ were calculated by averaging the bound ratio of the marker peaks. Data were plotted and fitted to a Hill method in OriginPro, and the function of the Hill method was:

$$\theta = \frac{x^n}{x^n + {k_d}^n}$$

, in which n denoted Hill coefficient. The average bound population increase from 0% at 10 mM [K^+] to 97% at 150 mM [K^+]. In the range of 50 mM to 100 mM [K^+], the major conformational transition takes place.

Electrophysiology. Freshly prepared T74S/H25R/E118A KcsA was prepared using former protocols and purified with a gravity Nickel column and desalting column on FPLC. 5 mg DOPE:DOPG 3:1 liposome were prepared: lipids in chloroform were dried under nitrogen gas, and pentane was added to get rid of all the organic solvents; dry lipids were resuspended by sonication in 1 ml HEPES swelling buffer while slowly adding CHAPS detergent to clear, in total 30mg CHAPS were added. 2.5 ug T74S/H25R/E118A KcsA was added into the liposome, and the mixture were incubated under room temperature for 30 mins. Bio-beads column was used to get rid of the detergent, and the proteoliposomes were eluted at 8 ml and frozen in liquid nitrogen.
Electrophysiology experiments were carried out with a partition diameter of 100 m. The lower chamber bath pH was at 4.0 (succinic acid buffer) and the upper chamber pH was at 7.0 (HEPES buffer, 100 mM K^+). Data were collected in Clampex and processed in Clampfit.

ACKNOWLEDGMENTS. We would like to acknowledge members of A.E.M.'s group: Dr. Rivkah Rogawski and Dr. Keith Fritzsching for insightful discussion. We thank Crina Nimigean of Cornell Weill University for assistance with the electrophysiology experiments. The NMR data were collected at the NYSBC with support from the Center on Macromolecular Dynamics by NMR Spectroscopy, a Biomedical Technology Research Resource supported by the NIH through Grant P41 GM118302. The NYSBC is also enabled by a grant from the Empire State Division of Science Technology and Innovation and by Office of Research Infrastructure Programs/NIH Facility Improvement Grant CO6RR015495. This work was supported by NIH Grant R01 GM088724 (to A.E.M).

1. Cuello LG, et al. (2010) Structural basis for the coupling between activation and inactivation gates in k(+) channels. *Nature* 466(7303):272–5.
2. McCoy JG, Nimigean CM (2012) Structural correlates of selectivity and inactivation in potassium channels. *Biochim Biophys Acta* 1818(2):272–85.
3. Zachariae U, et al. (2008) The molecular mechanism of toxin-induced conformational changes in a potassium channel: relation to c-type inactivation. *Structure* 16(5):747–54.
4. Alseikhan BA, DeMaria CD, Colecraft HM, Yue DT (2002) Engineered calmodulins reveal the unexpected eminence of ca2+ channel inactivation in controlling heart excitation. *Proc Natl Acad Sci U S A* 99(26):17185–90.
5. Faber ES, Sah P (2003) Ca2+-activated k+ (bk) channel inactivation contributes to spike broadening during repetitive firing in the rat lateral amygdala. *J Physiol* 552(Pt 2):483–97.
6. Cortes DM, Cuello LG, Perozo E (2001) Molecular architecture of full-length kcsa - role of cytoplasmic domains in ion permeation and activation gating. *Journal of General Physiology* 117(2):165–180.
7. Cuello LG, Romero JG, Cortes DM, Perozo E (1998) Proton-dependent gating in the streptomyces k+ channel. *Biophysical Journal* 74(2):A254–A254.
8. Heginbotham L, LeMasurier M, Kolmakova-Partensky L, Miller C (1999) Single streptomyces lividans k(+) channels: functional asymmetries and sidedness of proton activation. *J Gen Physiol* 114(4):551–60.
9. Heginbotham L, LeMasurier M, Kolmakova-Partensky L, Miller C (1999) Single streptomyces lividans k+ channels: Functional asymmetries and sidedness of proton activation. *Journal of General Physiology* 114(4):551–559.
10. Bhate MP, McDermott AE (2012) Protonation state of e71 in kcsa and its role for channel collapse and inactivation. *Proc Natl Acad Sci U S A* 109(38):15265–70.
11. Linder T, de Groot BL, Stary-Weinzinger A (2013) Probing the energy landscape of activation gating of the bacterial potassium channel kcsa. *PLoS Comput Biol* 9(5):e1003058.
12. Wylie BJ, Bhate MP, McDermott AE (2014) Transmembrane allosteric coupling of the gates in a potassium channel. *Proc Natl Acad Sci U S A* 111(1):185–90.
13. Xu Y, Bhate MP, McDermott AE (2017) Transmembrane allosteric energetics characterization for strong coupling between proton and potassium ion binding in the kcsa channel. *Proc Natl Acad Sci U S A* 114(33):8788–8793.
14. Cuello LG, Cortes DM, Jogini V, Sompornpisut A, Perozo E (2010) A molecular mechanism for proton-dependent gating in kcsa. *FEBS Lett* 584(6):1126–32.
15. Cuello LG, et al. (2010) Design and characterization of a constitutively open kcsa. *FEBS Lett* 584(6):1133–8.
16. Miloshevsky GV, Jordan PC (2007) Open-state conformation of the kcsa k+ channel: Monte carlo normal mode following simulations. *Structure* 15(12):1654–62.
17. Thompson AN, Posson DJ, Parsa PV, Nimigean CM (2008) Molecular mechanism of ph sensing in kcsa potassium channels. *Proc Natl Acad Sci U S A* 105(19):6900–5.
18. Takeuchi K, Takahashi H, Kawano S, Shimada I (2007) Identification and characterization of the slowly exchanging ph-dependent conformational rearrangement in kcsa. *J Biol Chem* 282(20):15179–86.
19. Posson DJ, Thompson AN, McCoy JG, Nimigean CM (2013) Molecular interactions involved in proton-dependent gating in kcsa potassium channels. *J Gen Physiol* 142(6):613–24.
20. Cuello LG, Cortes DM, Jogini V, Sompornpisut A, Perozo E (2010) A molecular mechanism for proton-dependent gating in kcsa. *Febs Letters* 584(6):1126–1132.
21. Cuello LG, et al. (2010) Structural basis for the coupling between activation and inactivation gates in k+ channels. *Nature* 466(7303):272–U154.
22. Imai S, Osawa M, Takeuchi K, Shimada I (2010) Structural basis underlying the dual gate properties of kcsa. *Proceedings of the National Academy of Sciences of the United States of America* 107(14):6216–6221.
23. Kim DM, et al. (2016) Conformational heterogeneity in closed and open states of the kcsa potassium channel in lipid bicelles. *Journal of General Physiology* 148(2):119–132.
24. Posson DJ, Thompson AN, McCoy JG, Nimigean CM (2013) Molecular interactions involved in proton-dependent gating in kcsa potassium channels. *Journal of General Physiology* 142(6):613–624.
25. Thompson AN, McCoy J, Posson D, Nimigean CM (2011) Molecular interactions involved in kcsa ph gating. *Biophysical Journal* 100(3):273–273.

26. Wylie BJ, Bhate MP, McDermott AE (2014) Transmembrane allosteric coupling of the gates in a potassium channel. *Proceedings of the National Academy of Sciences of the United States of America* 111(1):185–190.
27. Xu Y, Zhang D, Rogawski R, Nimigean CM, McDermott AE (2019) Identifying coupled clusters of allostery participants through chemical shift perturbations. *Proceedings of the National Academy of Sciences* p. 201811168.
28. Li J, Ostmeyer J, Cuello LG, Perozo E, Roux B (2018) Rapid constriction of the selectivity filter underlies c-type inactivation in the kcsa potassium channel. *J Gen Physiol* 150(10):1408–1420.
29. Cuello LG, Jogini V, Cortes DM, Perozo E (2010) Structural mechanism of c-type inactivation in k+ channels. *Nature* 466(7303):203–U73.
30. Xu YY, Bhate MP, McDermott AE (2017) Transmembrane allosteric energetics characterization for strong coupling between proton and potassium ion binding in the kcsa channel. *Proceedings of the National Academy of Sciences of the United States of America* 114(33):8788–8793.
31. Bhate MP, McDermott AE (2012) Protonation state of e71 in kcsa and its role for channel collapse and inactivation. *Proceedings of the National Academy of Sciences of the United States of America* 109(38):15265–15270.
32. Chakrapani S, Cordero-Morales JF, Perozo E (2007) A quantitative description of kcsa gating i: Macroscopic currents. *Journal of General Physiology* 130(5):465–478.
33. Cordero-Morales JF, Cuello LG, Perozo E (2006) Voltage-dependent gating at the kcsa selectivity filter. *Nature Structural & Molecular Biology* 13(4):319–322.
34. Thompson AN, Posson DJ, Parsa PV, Nimigean CM (2008) Molecular mechanism of ph sensing in kcsa potassium channels. *Proceedings of the National Academy of Sciences of the United States of America* 105(19):6900–6905.
35. Dart C (2010) Lipid microdomains and the regulation of ion channel function. *Journal of Physiology-London* 588(17):3169–3178.
36. Nakao H, et al. (2015) ph-dependent promotion of phospholipid flip-flop by the kcsa potassium channel. *Biochim Biophys Acta* 1848(1 Pt A):145–50.
37. Schmidt D, Jiang QX, MacKinnon R (2006) Phospholipids and the origin of cationic gating charges in voltage sensors. *Nature* 444(7120):775–9.
38. Valiyaveetil FI, Zhou YF, Mackinnon R (2002) Lipids in the structure, folding, and function of the kcsa k+ channel. *Biochemistry* 41(35):10771–10777.
39. Liu S, et al. (2015) Ion-binding properties of a k+ channel selectivity filter in different conformations. *Proc Natl Acad Sci U S A* 112(49):15096–100.
40. Otzen DE (2002) Protein unfolding in detergents: effect of micelle structure, ionic strength, ph, and temperature. *Biophys J* 83(4):2219–30.
41. Uysal S, et al. (2009) Crystal structure of full-length kcsa in its closed conformation. *Proceedings of the National Academy of Sciences of the United States of America* 106(16):6644–6649.
42. Morcombe CR, Zilm KW (2003) Chemical shift referencing in mas solid state nmr. *J Magn Reson* 162(2):479–86.
43. Takegoshi K, Nakamura S, Terao T (2001) C-13-h-1 dipolar-assisted rotational resonance in magic-angle spinning nmr. *Chemical Physics Letters* 344(5-6):631–637.
44. Takegoshi K, Nakamura S, Terao T (2003) C-13-h-1 dipolar-driven c-13-c-13 recoupling without c-13 rf irradiation in nuclear magnetic resonance of rotating solids. *Journal of Chemical Physics* 118(5):2325–2341.
45. Fung BM, Khitrin AK, Ermolaev K (2000) An improved broadband decoupling sequence for liquid crystals and solids. *Journal of Magnetic Resonance* 142(1):97–101.
46. Goddard T, D.G. K (year?) Sparky 3. *University of California, San Francisco.*

DRAFT